

Shallow learning enables real-time inference of molecular composition changes from broadband-near-infrared spectroscopy of brain tissue

IVAN EZHOV,^{1,*} LUCA GIANNONI,^{2,3} IVAN ILIASH,¹ FELIX HSIEH,¹
CHARLY CAREDDA,⁵ FRED LANGE,⁴ ILIAS TACHTSIDIS,⁴ AND DANIEL
RUECKERT^{2,3}

¹Technical University of Munich, Germany

²University of Florence, Italy

³European Laboratory for Non-Linear Spectroscopy, Italy

⁴University College London, United Kingdom

⁵Univ Lyon, INSA-Lyon, Université Claude Bernard Lyon 1, UJM-Saint Etienne, CNRS, Inserm, CREATIS UMR 5220, France

⁴Imperial College London, United Kingdom

*ivan.ezhov@tum.de

Abstract: Spectroscopy-based imaging modalities such as near-infrared spectroscopy (NIRS) and hyperspectral imaging (HSI) represent a promising alternative for low-cost, non-invasive, and fast monitoring of functional and structural properties of living tissue. Particularly, the possibility of extracting the molecular composition of the tissue from the optical spectra in real-time deems the spectroscopy techniques as unique diagnostic tools. However, due to the highly limited availability of paired optical and molecular profiling studies, building a mapping between a spectral signature and a corresponding set of molecular concentrations is still an unsolved problem. Moreover, there are no yet established methods to streamline inference of the biochemical composition from the optical spectrum for real-time applications such as surgical monitoring.

In this paper, we develop a technique for fast inference of changes in the molecular composition of brain tissue. We base our method on the Beer-Lambert law to analytically connect the spectra with concentrations and use a deep-learning approach to significantly speed up the concentration inference compared to traditional optimization methods. We test our approach on real data obtained from the broadband NIRS study of piglets' brains [Helicoid;MC]. The results demonstrate that the proposed method enables real-time molecular composition inference while maintaining the accuracy of traditional optimization.

1. Introduction

Various biomedical applications such as laboratory tissue examination or neurosurgery require access to rapid monitoring of intrinsic tissue properties. In particular, neuronavigation would benefit by having structural and functional information about brain matter in real-time [1–3]. Spatially-resolved maps of the tissue characteristics would allow bypassing invasive disease diagnostics, e.g., biopsy, which halt the operation. Instead, a surgical decision could be made during the operation, reducing its time and preserving a healthy brain.

Optical sensing, such as near-infrared spectroscopy (NIRS) and hyperspectral imaging (HSI), emerge as promising alternatives to address these clinical needs [4, 5]. These techniques can probe biological matter utilizing non-ionizing electromagnetic radiation within the visible and near-infrared ranges. The spectral instrumentation is inexpensive, portable, and allows for continuous monitoring at the bedside [6].

The overarching principle behind spectroscopy-based molecular characterization is to relate

the reflection spectrum obtained upon illumination of the tissue surface with its optical properties. The molecules constituting the tissue have unique absorption dependency on the radiation frequency, and thus, the reflection should exhibit molecular absorption signatures in its frequency dependency.

However, several other physical factors contribute to shaping the spectra. These include light scattering on the surface and within tissue volume, autofluorescence, and background illumination [7]. Disentangling these phenomena from a reflectance spectrum is often an ambiguous, ill-posed problem, yet it is crucial for deducing the relation between the reflection and molecular composition. Another complication is a scarcity of available studies in which both optical monitoring and biochemical composition analysis are performed at the same time.

Analytical and statistical approaches exist aiming to unmix optical spectra into the physical phenomena defining the spectra profile under a limited data regime [8–13]. The first family of methods mitigates the data scarcity by introducing a physical prior to establish the spectrochemical link. Typically, the Beer-Lambert law [14] is used to provide such a link by describing the incoming light's energy dissipation as an exponentially decaying function of light penetration depth into the tissue:

$$\log(I_R(\lambda)/I_0(\lambda)) = - \left[\sum_i c_i \mu_a^i(\lambda) + s \mu_s(\lambda) \right] \cdot l + U \quad (1)$$

Here, $I_R(\lambda)$ and $I_0(\lambda)$ are the intensities of the reflected and the incoming light, μ_a and μ_s is the absorption and scattering coefficients, the index i denotes the molecule constituting the tissue such as water, fat, hemoglobin or cytochromes, c_i denotes the corresponding concentration, and s is the weight of scattering in the total light energy dissipation. The remaining quantities are λ , which is the light wavelength, l is the light penetration depth, and U describes other physical factors contributing to the energy dissipation of the incoming light, such as autofluorescence, or other sources of the optical signal captured by the cameras such as ambient illumination. Now, in the case of changes in molecular composition over the course of optical monitoring, one can assume that the effects contributing to U either stay constant (e.g., which is a fair assumption for ambient illumination) or change notably less than the total absorption ¹. Under this assumption, subtraction of two reflection spectra, $\log I_R^2 - \log I_R^1$, would cancel out or make negligible the term $\delta U = U^2 - U^1$ in the following equation:

$$\log(I_R^2(\lambda)/I_R^1(\lambda)) = - \left[\sum_i \delta c_i \mu_a^i(\lambda) + \delta(s \mu_s(\lambda)) \right] \cdot l + \delta U, \quad (2)$$

In such a differential form, the Beer-Lambert law can now be used to identify molecular composition. For this, standard least-squares optimization algorithms can be employed to minimize the difference between the real spectra and the spectra obtained from the Beer-Lambert law. As a result of the minimization, the optimal values of the set of concentration changes $\{\delta c_i = c_i^2 - c_i^1\}$ are obtained (alongside the scattering parameters if the phenomenon is taken into consideration).

Another family of unmixing approaches is based on statistical techniques such as principal component analysis (PCA) [11–13]. Here, by analyzing through the PCA, a large dataset of reflection spectra, one identifies the importance of each wavelength to explain the variance in the dataset. Assuming that from the physics point of view, the variance in the reflection spectra is mainly due to varying molecular absorption, one can try to correlate the output of the PCA analysis with the absorption spectra. In [11], the authors discuss how such correlation can reveal the relative difference in concentration of chromophores.

¹In certain scenarios, even changes in scattering are not expected since it is a rather bulk effect dependent on the density of the probed matter rather than molecule-specific one.

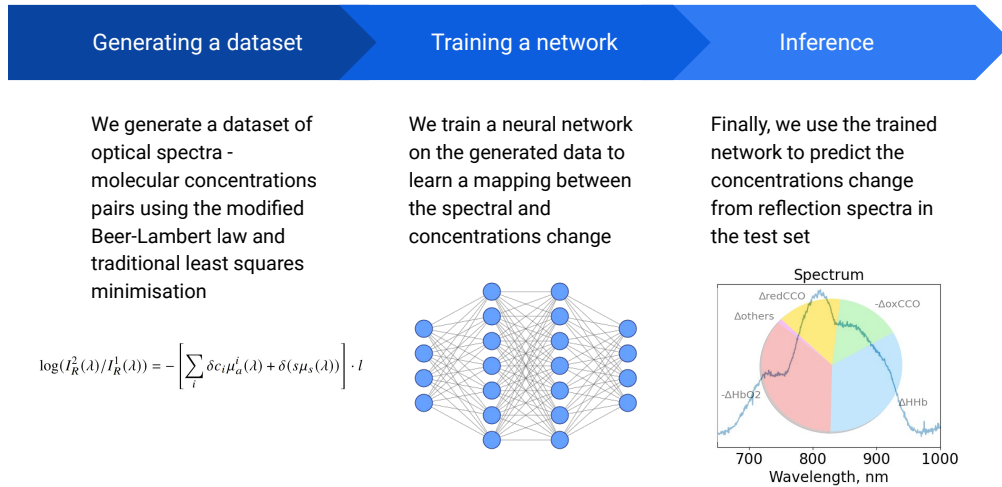


Fig. 1. The general pipeline describing our approach for inferring molecular concentrations' changes $\{\delta c_i\}$ from changes in the reflection spectra.

The overarching drawback of these approaches is the computational time it takes to infer the biochemical composition. For example, the optimization methods take a subsecond time to infer the composition of a single spectrum containing typical for NIRS and HSI number of wavelengths (a few hundred). However, when using modalities providing spatially-resolved imaging for real-time applications, one needs to solve the optimization task in a subsecond time for as many spectra as there are spatial pixels, as every pixel contains its own spectrum. For modalities like HSI, the number of pixels can be easily in the order of 10^5 . Providing subsecond timings for simultaneous inference on such an amount of spectra poses a challenge for traditional methods ².

The present paper aims to alleviate the computational time limitation of existing methods by proposing a data-driven solution that significantly speeds up the biochemical composition inference. We test two types of deep-learning-based approaches which differ in the way the training dataset is collected: a) directly by generating synthetic spectrum-concentrations pairs from the Beer-lambert law or b) by inferring the molecular composition from real spectra by means of the traditional optimization and then use the pairs of real spectra and inferred concentrations for a neural network training. We evaluate the method on broadband NIRS data of piglets brain [15] and achieve a significant speed-up compared to the convex least-squares optimization while maintaining its accuracy. To our knowledge, this is the first work that applies a neural-network-based approach to provide real-time chromophore composition inference from spectroscopy measurements [16–23].

2. Method

As mentioned in the introduction, inference of absolute chromophore concentrations from an optical spectrum is a challenging task due to multiple physical effects shaping the reflection spectrum. Thus, we instead aim to predict the changes in concentrations from changes in the spectrum upon temporal brain matter monitoring, Eq. 2.

²Note that under assumption of negligible contribution from scattering in the modified Beer-Lambert law, the Eq. 2 results in a linear system. Such system can be efficiently solved using the pseudoinverse achieving close to real-time computation.

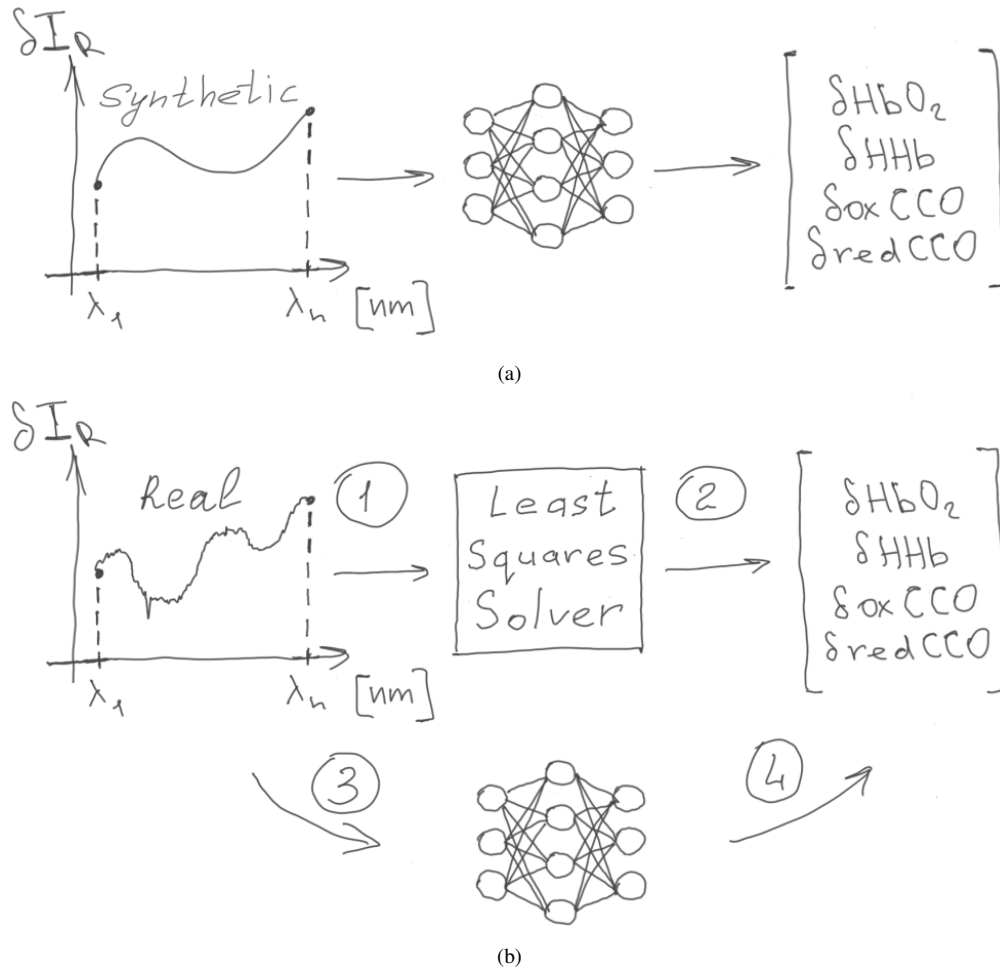


Fig. 2. Two strategies for collecting the training dataset. Strategy (a) in which we train a network on synthetic spectra-concentration pairs generated from the modified Beer-Lambert law. Strategy (b) in which the training is performed on pairs of real spectra and concentrations obtained through the least-squares fit to the corresponding real spectra.

Datasets creation. In our method, we use a supervised data-driven approach by creating a dataset of spectra-concentration pairs to train a neural network. We employ two different strategies to create the dataset:

a) The first strategy directly utilizes the Beer-Lambert law to generate the training dataset pairs. We randomly sample values for two sets of the molecular composition $\{c_i^1\}$ and $\{c_i^2\}$ using the Dirichlet distribution for each. Such distribution ensures the physiological plausibility as the concentrations of molecules should sum up to one, $\sum_i c_i^j = 1$. If scattering is included in Eq. 2, the corresponding parameters s and b in the rational function $s\lambda^{-b}$ describing the scattering process are sampled as well [24]. Subsequently, we independently input these two sets of values into the Beer-Lambert law to obtain the synthetic reflection spectra. The difference in spectra $\delta I_R = I_R^2 - I_R^1$ and corresponding $\{\delta c_i\}$ (plus s and b in the scattering case) are used for the training.

b) Given that the distribution of the synthetic spectra obtained according to the strategy

described above can be notably different from the distribution of real spectra, this can result in an unsatisfactory network prediction accuracy. Therefore, in addition to (a), we evaluate another strategy for creating a dataset trying to bridge the gap between the physical model and real data. For this, we use traditional least squares minimization to fit the changes in the real reflectance spectrum with a synthetic spectrum difference obtained from the modified Beer-Lambert law. The concentrations $\{\delta c_i\}$ (optionally with s and b) found upon the optimization and the corresponding δI_R constitute the training samples.

Network and optimization details. The training was performed using the multi-layer perceptron (MLP) neural network for both datasets. The MLP architecture with an exponential Linear Unit activation function. The network takes as input a one-dimensional vector of spectra difference and outputs four concentration changes for oxyhemoglobin, deoxyhemoglobin, oxidase and reduced cytochrome-c-oxidase $\{\delta c_{HbO_2}, \delta c_{HHb}, \delta c_{oxCCO}, \delta c_{redCCO}\}$ (the contribution of water and fat can be assumed negligible in the considered range of wavelength between 760 and 900 nm [15, 25]). We trained both networks with early stopping when they reached convergence.

In order to perform the least-squared optimization on real spectra, we used a publicly available solver for convex quadratic programs [26] from the *cvxpy* library [27]. The average computing time for solving the linear system derived from the Beer-Lambert law for a single spectrum with 140 wavelengths (i.e., 140 equations in the linear system) is, on average, ca. 6 ms on a machine with eight Intel i7-1165G7 cores and 16GB RAM. Since the total concentration of cytochrome-c-oxidase can be considered nearly constant during the experiment [28], we incorporate this biological knowledge into the optimization by adding a constrain $|\delta c_{oxCCO} + \delta c_{redCCO}| \leq 0.01$.

3. Results

Data. For our experiments, we used broadband NIRS spectral data from a study analyzing 27 piglets’ brains in which a hypoxia state was induced [15]. The piglets were monitored for several hours, during which the carotid arteries were surgically isolated. This allowed controlling the blood flow to the brain. The details of the intervention protocol are described in [15]. The measurements contain around eight thousand spectra per piglet. We normalized the spectra with respect to dark noise and white reference. The normalized NIRS spectra before and after the intervention inducing hypoxia are shown in Fig. 3 (left), and predictions of the concentrations change over the course of the optical monitoring using the least-squares optimization are shown in Fig. 3 (right). We used the least-squares minimization predictions as the ground truth to validate all the trained networks. Out of 27 piglets, 17 were used for training, and the remaining ones - for validation and testing.

Experiments. Fig. 4 demonstrates the results of the experiment in which we test the network trained on synthetic data collected according to strategy (a). Even though the predictions for both hemoglobin and cytochrome-c-oxidase are within expectations (as cytochrome reduction reaction is supposed to be less active and deoxyhemoglobin should increase with a decrease of oxygen [29, 30]), the network predictions are notably off with respect to the ground truth. This behavior is also within our expectations as the distribution of synthetic data on which the network was trained and real data on which it was evaluated notably vary (as shown in Fig. 4 by using the principal component analysis for comparing the two distributions).

Fig. 5 demonstrates the results of the experiment in which we test the network trained on real data. In contrast to the synthetic data case, the network infers molecular composition almost identical to the convex optimization solver.

Importantly, this comes with a significant computational time speed up. In Fig. 6, we show the ablation analysis on how much the network’s inference time (as well as accuracy) changes upon varying the depth (number of hidden layers) and the width (number of neurons in a layer)

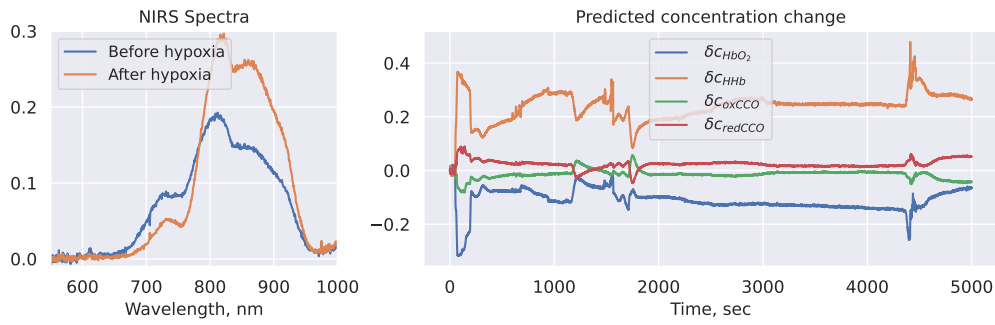


Fig. 3. Optical spectra from the broadband NIRS study in [15] before and after inducing hypoxia in the piglet's brain (left). On the right, predictions of the molecular concentration change $\{\delta C_{HbO_2}, \delta C_{Hb}, \delta C_{oxCCO}, \delta C_{redCCO}\}$ over the course of the optical monitoring using the least-squares optimization.

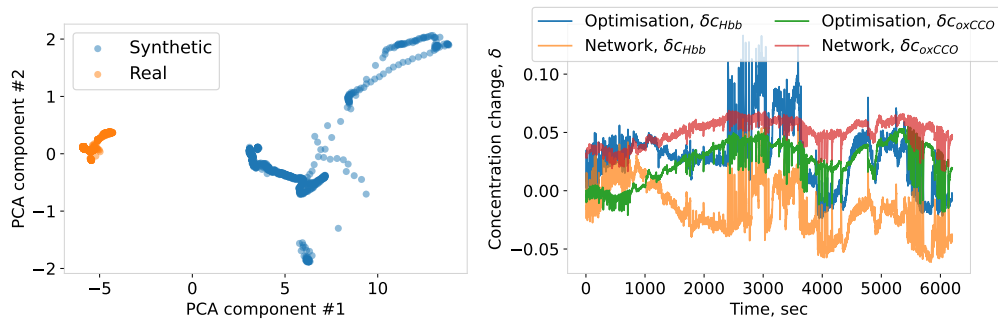


Fig. 4. Visualisation of the synthetic and real spectra distributions using the first two components of the PCA statistical tool (left) and predictions of the network trained on synthetic data (right). The notable difference in spectral data distribution results in unsatisfactory network performance.

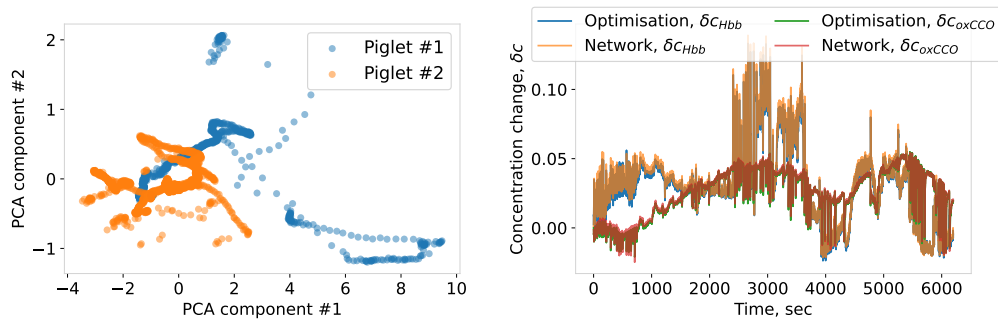


Fig. 5. Visualisation of the difference across real spectra distribution using PCA method (left) and predictions of the network trained on real data according to strategy (b) for the dataset collection (right). The network performance is significantly better than the performance of the network trained on synthetic data.

in the network architecture. As one can see, it takes ca. 200 ms for the largest network (and ca. 25 ms for the smallest one) to infer biochemical composition for 10^5 spectra. This is significantly

faster than convex optimization which takes up to one minute to infer an analogous amount of optical spectra (importantly, the time for the optimization method was achieved by parallelizing computation, i.e. concentrations for all spectra were obtained at the same time by solving the linear system). Also note, the experiments show that for the differential Beer-Lambert law without scattering, we achieve better accuracy on using a 1-layer network, compared to networks with more layers. We attribute it to the fact that when scattering is not included, we try to approximate a solution to a linear system. Therefore having a network with multiple layers, i.e. multiple non-linearities, is prone to the network overfitting on the training data, solutions of a linear system.

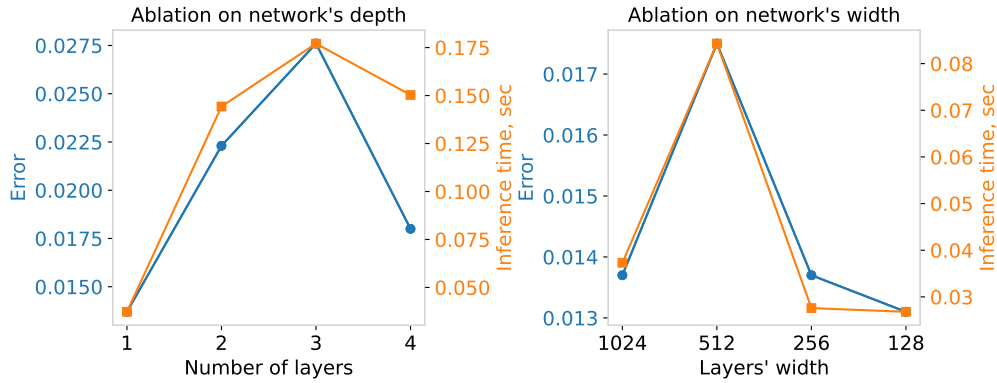


Fig. 6. Ablation analysis on the network's depth (left) and network's width (right). For the depth ablation, we used 1024 neurons per layer. For the width ablation, we used a network with a single hidden layer. The chromophore composition's inference time for the largest network is around 200 ms for 10^5 spectra which is orders of magnitude faster than traditional optimization.

4. Conclusion

In the paper, we present proof of a data-driven concept for inferring molecular composition change from spectra of living tissue. We test the approach on broadband NIRS data of piglets whose brains were optically monitored while hypoxia was induced in the cerebral tissue. We achieve a significant speed-up compared to traditional least-squares optimization, reaching subsecond time for inferring molecular composition. This timing would allow for real-time tissue characterization for both NIRS and HSI imaging. However, translating this approach to clinical or laboratory use requires validating the method on tissue samples for which the biochemical composition is known (e.g., tissue phantoms) and, as a likely consequence, investigating the limits of the modified Beer-Lambert law applicability [14, 31].

References

1. O. Ganslandt, S. Behari, J. Gralla, R. Fahlbusch, and C. Nimsky, "Neuronavigation: concept, techniques and applications." *Neurol. India* **50**, 244 (2002).
2. D. A. Orringer, A. Golby, and F. Jolesz, "Neuronavigation in the surgical management of brain tumors: current and future trends," *Expert review medical devices* **9**, 491–500 (2012).
3. I. J. Gerard, M. Kersten-Oertel, J. A. Hall, D. Sirhan, and D. L. Collins, "Brain shift in neuronavigation of brain tumors: an updated review of intra-operative ultrasound applications," *Front. Oncol.* **10**, 618837 (2021).
4. A. N. Sen, S. P. Gopinath, and C. S. Robertson, "Clinical application of near-infrared spectroscopy in patients with traumatic brain injury: a review of the progress of the field," *Neurophotonics* **3**, 031409–031409 (2016).
5. L. Giannoni, F. Lange, and I. Tachtsidis, "Hyperspectral imaging solutions for brain tissue metabolic and hemodynamic monitoring: past, current and future developments," *J. Opt.* **20**, 044009 (2018).

6. D. Viderman and Y. G. Abdildin, "Near-infrared spectroscopy in neurocritical care: a review of recent updates," *World Neurosurg.* **151**, 23–28 (2021).
7. G. Lu and B. Fei, "Medical hyperspectral imaging: a review," *J. biomedical optics* **19**, 010901–010901 (2014).
8. S. Tzoumas and V. Ntziachristos, "Spectral unmixing techniques for optoacoustic imaging of tissue pathophysiology," *Philos. Trans. Royal Soc. A: Math. Phys. Eng. Sci.* **375**, 20170262 (2017).
9. N. Dobleon, Y. Altmann, N. Brun, and S. Moussaoui, "Linear and nonlinear unmixing in hyperspectral imaging," in *Data Handling in Science and Technology*, vol. 30 (Elsevier, 2016), pp. 185–224.
10. G. Lu, X. Qin, D. Wang, Z. G. Chen, and B. Fei, "Estimation of tissue optical parameters with hyperspectral imaging and spectral unmixing," in *Medical Imaging 2015: Biomedical Applications in Molecular, Structural, and Functional Imaging*, vol. 9417 (SPIE, 2015), pp. 199–205.
11. I. Ezhov, L. Giannoni, S. Shit, F. Lange, F. Kofler, B. Menze, I. Tachtsidis, and D. Rueckert, "Identifying chromophore fingerprints of brain tumor tissue on hyperspectral imaging using principal component analysis," arXiv preprint arXiv:2301.05233 (2023).
12. K. Yokoyama, M. Watanabe, and E. Okada, "Estimation of the optical path length factor for functional imaging of an exposed cortex by principal component analysis," in *European Conference on Biomedical Optics*, (Optica Publishing Group, 2003), p. 5138_168.
13. A. O. Gerstner, W. Laffers, F. Bootz, D. L. Farkas, R. Martin, J. Bendix, and B. Thies, "Hyperspectral imaging of mucosal surfaces in patients," *J. biophotonics* **5**, 255–262 (2012).
14. I. Oshina and J. Spigulis, "Beer–lambert law for optical tissue diagnostics: current state of the art and the main limitations," *J. biomedical optics* **26**, 100901–100901 (2021).
15. P. Kayezhad, S. Mitra, G. Bale, C. Bauer, I. Lingam, C. Meehan, A. Avdic-Belltheus, K. A. Martinello, A. Bainbridge, N. J. Robertson *et al.*, "Quantification of the severity of hypoxic-ischemic brain injury in a neonatal preclinical model using measurements of cytochrome-c-oxidase from a miniature broadband-near-infrared spectroscopy system," *Neurophotonics* **6**, 045009–045009 (2019).
16. M. Mamouei, K. Budidha, N. Baishya, M. Qassem, and P. Kyriacou, "An empirical investigation of deviations from the beer–lambert law in optical estimation of lactate," *Sci. Reports* **11**, 13734 (2021).
17. P.-H. Chou, Y.-H. Yao, R.-X. Zheng, Y.-L. Liou, T.-T. Liu, H.-Y. Lane, A. C. Yang, and S.-C. Wang, "Deep neural network to differentiate brain activity between patients with first-episode schizophrenia and healthy individuals: a multi-channel near infrared spectroscopy study," *Front. psychiatry* **12**, 655292 (2021).
18. X. Y. Yap, K. S. Chia, and N. A. S. Suarin, "Adaptive artificial neural network in near infrared spectroscopy for standard-free calibration transfer," *Chemom. Intell. Lab. Syst.* **230**, 104674 (2022).
19. N. K. Qureshi, F. M. Noori, A. Abdullah, and N. Naseer, "Comparison of classification performance for fnirs-bci system," in *2016 2nd International Conference on Robotics and Artificial Intelligence (ICRAI)*, (IEEE, 2016), pp. 54–57.
20. Y. Karamavuş and M. Özkan, "Newborn jaundice determination by reflectance spectroscopy using multiple polynomial regression, neural network, and support vector regression," *Biomed. Signal Process. Control.* **51**, 253–263 (2019).
21. H. Bian, H. Yao, G. Lin, Y. Yu, R. Chen, X. Wang, R. Ji, X. Yang, T. Zhu, and Y. Ju, "Multiple kinds of pesticides detection based on back-propagation neural network analysis of fluorescence spectra," *IEEE Photonics J.* **12**, 1–9 (2020).
22. M. Ewerlöf, T. Strömberg, M. Larsson, and E. G. Salerud, "Multispectral snapshot imaging of skin microcirculatory hemoglobin oxygen saturation using artificial neural networks trained on in vivo data," *J. Biomed. Opt.* **27**, 036004–036004 (2022).
23. Z. Zhou, L. Zhao, X. Zhang, F. Cui, and L. Guo, "Real-time in-situ optical detection of fluid viscosity based on the beer-lambert law and machine learning," *Opt. Express* **30**, 41389–41398 (2022).
24. S. L. Jacques, "Optical properties of biological tissues: a review," *Phys. Med. & Biol.* **58**, R37 (2013).
25. L. Giannoni, F. Lange, and I. Tachtsidis, "Investigation of the quantification of hemoglobin and cytochrome-c-oxidase in the exposed cortex with near-infrared hyperspectral imaging: a simulation study," *J. biomedical optics* **25**, 046001 (2020).
26. B. Stellato, G. Banjac, P. Goulart, A. Bemporad, and S. Boyd, "OSQP: an operator splitting solver for quadratic programs," *Math. Program. Comput.* **12**, 637–672 (2020).
27. S. Diamond and S. Boyd, "CVXPY: A Python-embedded modeling language for convex optimization," *J. Mach. Learn. Res.* **17**, 1–5 (2016).
28. C. Kolyva, A. Ghosh, I. Tachtsidis, D. Highton, C. E. Cooper, M. Smith, and C. E. Elwell, "Cytochrome c oxidase response to changes in cerebral oxygen delivery in the adult brain shows higher brain-specificity than haemoglobin," *Neuroimage* **85**, 234–244 (2014).
29. M. Smith, "Shedding light on the adult brain: a review of the clinical applications of near-infrared spectroscopy," *Philos. Trans. Royal Soc. A: Math. Phys. Eng. Sci.* **369**, 4452–4469 (2011).
30. G. Bale, C. E. Elwell, and I. Tachtsidis, "From jöbssis to the present day: a review of clinical near-infrared spectroscopy measurements of cerebral cytochrome-c-oxidase," *J. biomedical optics* **21**, 091307–091307 (2016).
31. L. Kocsis, P. Herman, and A. Eke, "The modified beer–lambert law revisited," *Phys. Med. & Biol.* **51**, N91 (2006).